THE JOURNAL OF COMPARATIVE NEUROLOGY 319:205–217 (1992)

Limbic Thalamus in Rabbit: Architecture, Projections to Cingulate Cortex and Distribution of Muscarinic Acetylcholine, $GABA_A$, and Opioid Receptors

LESLIE J. VOGT, BRENT A. VOGT, AND ROBERT W. SIKES
Department of Physiology and Pharmacology, Bowman Gray School of Medicine, Wake Forest University, Winston-Salem, North Carolina 27103 (L.J.V., B.A.V.); Department of Physical Therapy, Northeastern University, Boston, Massachusetts 02118 (R.W.S.)

ABSTRACT

Nuclei of the thalamus that project to cingulate cortex have been implicated in responses to noxious stimuli, cholinergic and motor functions. The rabbit limbic thalamus may play an important role in these functions, but has not been studied extensively in terms of its cytoarchitecture, the topographical organization of its cortical projections, and differential transmitter regulation of its subnuclei. Therefore, the architecture, projections to cingulate cortex, and radioligand binding were investigated in the anterior, ventral, lateral, and midline nuclei of rabbit thalamus. The anterior nuclei are highly differentiated because both the dorsal and ventral nuclei have parvicellular and magnocellular divisions. Fluorescent dyes were injected into cingulate cortex to evaluate limbic thalamocortical connections. The anterior medial, submedial, and parafascicular nuclei project primarily to anterior cingulate cortex, while they have small or no projections to posterior areas. The ventral anterior and ventral lateral nuclei have a significant projection to dorsal cingulate cortex, including areas 24b and 29d. Projections of the anterior ventral nucleus are topographically organized, since medial parts of the parvicellular division project to rostral area 29, and lateral parts project to caudal area 29. The lateral nuclei and the parvicellular and magnocellular divisions of the anterior dorsal nucleus project with progressively higher densities in the rostrocaudal plane of area 29. Finally, the magnocellular division of the anterior ventral nucleus projects almost exclusively to caudal and ventral area 29, i.e., granular retrosplenial cortex. Ligand binding studies employed coverslip autoradiography and single grain counting techniques. Muscarinic receptor binding was moderate for both pirenzepine and oxotremorine-M in the parvicellular anterior ventral nucleus, while in other nuclei, there was an inverse relationship in the binding for these ligands. Most notably, the anterior dorsal nucleus, which receives no cholinergic input, had very high oxotremorine-M and low pirenzepine binding, while the anterior medial nucleus, which receives a moderate cholinergic input, had the highest pirenzepine binding and very low oxotremorine-M binding. Muscimol binding to $GABA_A$ receptors was highest in the anterior ventral nucleus, while it was at moderate levels in the anterior dorsal and lateral nuclei. The binding of Tyr-D-Ala-Gly-MePhe-Gly-ol to mu opioid receptors and 2-D-penicillamine-5-D-penicillamine-enkephalin to delta opioid receptors were both high in the parvicellular and low in the magnocellular divisions of the anterior dorsal nucleus. The magnocellular division of the anterior ventral, the lateral dorsal, and the parafascicular nuclei had high mu opioid binding, while the lateral dorsal and lateral magnocellular nuclei had low levels of delta opioid binding. The submedial nucleus had moderate binding of both opioid compounds. These results suggest that the limbic thalamus in the rabbit is highly differentiated and has topographically organized connections to cingulate cortex. Some of these connections may mediate responses to noxious stimuli including those from the submedial and parafascicular nuclei. Finally, the ligand

Accepted December 18, 1991.

Address reprint requests to Leslie J. Vogt, Dept. of Physiology and Pharmacology, Bowman Gray School of Medicine, Wake Forest University, 300 South Hawthorne Road, Winston-Salem, NC 27103.

binding studies indicate that transmitter systems differentially regulate the various subnuclei within the limbic thalamus and may modulate different components of limbic thalamocortical circuitry.

Key words: limbic system, muscimol, cholinergic receptors, enkephalin receptors, thalamic nuclei

The nuclei in the thalamus that have projections mainly to limbic cortex are referred to as the limbic thalamic nuclei. Cingulate cortex is one of the largest components of limbic cortex and it receives most input from the anterior, lateral, midline, and intralaminar thalamic nuclei (Rose and Woolsey, '48; Domesick, '72; Vogt et al., '79, '87; Matsuoka, '86; Sripanidkulchai and Wyss, '86; Minciacchi et al., '86; Horikawa et al., '88; Musil and Olson, '88; Buchanan et al., '89). Some of these nuclei have been implicated in responses to noxious stimuli. Thus, lesions in the parafascicular-centromedianum complex interfere with avoidance responses to noxious electrical stimulation of the tooth pulp in cats (Kaelber et al., '75), and ablations of the anterior and medial dorsal nuclei disrupt avoidance learning in rabbits where noxious footshock is the unconditional stimulus (Gabriel et al., '88). Electrophysiological studies have shown that neurons in the parafascicular, central lateral, and submedial nuclei respond to noxious mechanical and thermal stimuli (Casey, '66; Dong et al., '78; Peschanski et al., '81; Miletic and Coffield, '89). Furthermore, there are enkephalin-immunoreactive processes and neurons (Sar et al., '78; Finley et al., '81), and mu and delta opioid receptors in this part of the thalamus (Moskowitz and Goodman, '84; McLean et al., '86; Mansour et al., '87; Sharif and Hughes, '89). Since these nuclei project to anterior cingulate cortex (Jones and Leavitt, '74; Macchi et al., '77; Herkenham, '78; Vogt et al., '79, '87; Robertson and Kaitz, '81; Craig et al., '82; Royce and Mourey, '85; Royce et al., '89), they provide a potential source of nociceptor input to cingulate cortex and may be differentially regulated by opioid compounds and other neurotransmitters.

There is evidence for the differential regulation of thalamocortical projection neurons in limbic thalamus by cholinergic and GABAergic afferents. Thus, the parvicellular division of the anterior ventral nucleus has one of the highest levels of choline acetyltransferase immunoreactivity in the rodent thalamus, while there is no such immunoreactivity in the anterior dorsal nucleus (Levey et al., '87). Although all anterior nuclei have high and almost equivalent levels of binding of classical muscarinic antagonists (Kobayashi et al., '78; Rotter et al., '79), pirenzepine binding is highest in the parvicellular portion of the anterior ventral nucleus (Sikes and Vogt, '87), suggesting that cholinergic afferents differentially regulate divisions of the anterior nuclei. Additionally, Palacios et al. ('81) demonstrated that there are more high-affinity GABA receptors in the anterior ventral and anterior medial nuclei than in the anterior dorsal nucleus, suggesting that there are also differences in GABAergic control of limbic thalamic nuclei.

A survey of the cytoarchitecture of limbic thalamic nuclei in the rabbit brain suggests that these nuclei are highly differentiated. The anterior dorsal nucleus, for example, has parvicellular and magnocellular divisions which have not been previously described. Therefore, the present study was undertaken to analyze the structure of these nuclei in rabbit thalamus as well as the topographical organization of their projections to cingulate cortex. Since there is almost no information available about the distribution of transmitter receptors in the rabbit limbic thalamus, a combination of radioligand binding and coverslip autoradiography were used to assess the distribution of mu and delta opioid, muscarinic and $GABA_A$ receptors. These data in combination with the connection studies suggest that opioidergic, cholinergic, and GABAergic connections target different components of the limbic thalamic nuclei and so differentially regulate thalamocortical projection neurons.

MATERIALS AND METHODS

Nissl staining techniques

Five male Dutch belted rabbits were used for cytoarchitectural analysis of the limbic thalamus. The rabbits were overdosed with an i.p. injection of a mixture of chloral hydrate and pentobarbital (Chloropent, Fort Dodge Laboratories, Fort Dodge, IA; 3.5 ml/kg) and perfused briefly with 500 ml 0.9% saline followed by 1 liter of 10% formalin. The brains were removed, celloidin embedded and cut at a thickness of 40 μm. The sections were then stained with cresyl violet. The cytoarchitecture of nuclei in limbic thalamus were delineated according to the criteria of Gerhard ('68), Rose and Woolsey ('48), and Vogt and Sikes ('90).

Fluorescent tracer techniques

Fluorescent dyes were injected into the cingulate cortices of 19 rabbits. The rabbits were anesthetized with an i.p. injection of a mixture of ketamine and xylazine (Bristol

Abbreviations

AD	anterior dorsal nucleus
ADm	anterior dorsal nucleus, magnocellular division
ADp	anterior dorsal nucleus, parvicellular division
AM	anterior medial nucleus
AV	anterior ventral nucleus
AVm	anterior ventral nucleus, magnocellular division
AVp	anterior ventral nucleus, parvicellular division
Ce	central nucleus
CL	central lateral nucleus
LD	lateral dorsal nucleus
LM	lateral magnocellular nucleus
LP	lateral posterior nucleus
MD	medial dorsal nucleus
MDm	medial dorsal nucleus, magnocellular division
MDp	medial dorsal nucleus, parvicellular division
MTT	mamillothalamic tract
Pf	parafascicular nucleus
Pt	paratenial nucleus
Pv	paraventricular nucleus
Re	reuniens nucleus
Rh	rhomboid nucleus
Sm	stria medullaris
SM	submedial nucleus
VA	ventral anterior nucleus
VB	ventral basal nucleus
VL	ventral lateral nucleus
VM	ventral medial nucleus

Laboratories, Syracuse, NY; 35 mg ketamine and 5 mg xylazine/kg; White and Holmes, '76). Diamidino yellow (0.1 μl; 3% w/v in distilled water; Keizer et al., '83), fast blue (7% w/v in distilled water) or rhodamine-labeled fluorescent latex microspheres (Katz et al., '84) were injected through glass micropipettes. The animals were perfused 5–7 days after the injections with 500 ml 0.9% saline followed by 1 liter of 10% formalin in 0.1 M cacodylate buffer. The brains were removed, placed in 30% sucrose in cacodylate buffer until they sank, and then cut into 40-μm-thick sections on a freezing microtome. One series of sections (1 in 6) was stained with thionin and an unstained series (1 in 6) was dehydrated and coverslipped.

Brightfield illumination and epifluorescence (fast blue and diamidino yellow: 380–425-nm excitation, 450-nm absorption; rhodamine microspheres: 546-nm excitation, 580-nm absorption) were used to determine cytoarchitecture and to visualize labeled neurons, respectively. The cytoarchitectural areas in cingulate cortex were defined according to the criteria of Vogt et al. ('86). Injection sites were plotted onto a flattened map of these areas as shown in Figure 3. The labeled neurons were plotted with an IBM AT computer interfaced to the x and y coordinates of the microscope stage. Thalamic nuclei in adjacent thionin-stained sections were plotted to determine the locations of labeled neurons in the unstained sections. Neurons in every unstained section were plotted, and labeled neurons counted in each nucleus. In the figures, each dot represents 4 labeled neurons. Labeled neurons in limbic thalamus for each case were totalled and the percentage of labeled neurons in each nucleus was calculated. These percentages, as well as the total number of labeled neurons counted, are presented in Table 1.

Ligand binding techniques

A total of 18 male Dutch belted and New Zealand rabbits were used for ligand binding studies. They were sacrificed with CO_2, their brains were removed, the thalamus dissected, and frozen to −80°C. Cryostat sections 30-μm-thick were cut and mounted on chrom-alum coated slides.

Unlabelled pirenzepine was kindly provided by Boehringer Ingelheim, Ltd. and levallorphan was kindly provided by Hoffmann-La Roche. Tritiated ligands were purchased from New England Nuclear. Muscarinic receptor binding was assayed by autoradiography with [^{3}H]pirenzepine (specific activity 84 Ci/mM) and [^{3}H]oxotremorine-M (specific activity 85.1 Ci/mM). For the pirenzepine binding assay, sections were incubated in 12 nM [^{3}H]pirenzepine in Krebs-Henseleit buffer for 70 minutes at 25°C, followed by 2 buffer washes at 4°C for 3 minutes each, and the sections were then quickly air dried. Non-specific binding was determined with 1 μM atropine in a parallel series of sections. Binding of [^{3}H]oxotremorine-M involved incubation of sections for 30 minutes at 25°C in 0.1 nM [^{3}H]oxotremorine-M in 20 mM Hepes-Tris buffer with 10 mM Mg^{2+} and 50 nM pirenzepine (OXO-M/PZ). Sections were then washed in buffer at 4°C for 2 minutes each followed by a 2 minute water wash. Sections were then quickly air dried. Non-specific binding was assessed in a parallel series with 1 μM atropine.

[^{3}H]muscimol binding (specific activity 23.2 Ci/mM) was assessed in sections that were preincubated in 50 mM Tris buffer for 40 minutes at 20°C. Sections were then incubated for 15 minutes at 20°C in buffer with 20 nM [^{3}H]muscimol, followed by one buffer wash for 2 minutes at 4°C and a 2 minute water wash at 4°C and then were quickly air dried. Non-specific binding was determined by coincubation with 100 μM muscimol.

Mu and delta opioid receptor binding was analyzed by using [^{3}H]Tyr-D-Ala-Gly-MePhe-Gly-ol (DAGO; specific activity 30.3 Ci/mM) and [^{3}H]2-D-penicillamine-5-D-penicillamine-enkephalin (DPDPE; specific activity 43 Ci/mM), respectively. For the DAGO binding assay, sections were incubated for 45 minutes at 25°C in 50 mM Tris with 1 nM [^{3}H]DAGO. Sections were then washed in buffer three times for 1 minute each at 4°C and quickly air dried. Non-specific binding was evaluated in a parallel series with 1 μM levallorphan. Binding of DPDPE involved preincubation of sections in 50 mM Tris with 5 mM $MgCl_2$, 2 mg/ml bovine serum albumin, 20 μg/ml bacitracin, 100 mM NaCl and 50 μM GTP for 15 minutes at 25°C, followed by two 5 minute washes at 25°C in buffer to remove the GTP. The sections were then incubated for 1 hour at 25°C in 50 mM Tris with 2 mg/ml bovine serum albumin and 5 nM [^{3}H]DPDPE. The incubation was followed by three buffer washes for 10 minutes each at 4°C and the sections were then quickly air dried. Non-specific binding was determined with 1 μM DPDPE.

The method of Young and Kuhar ('79) was used to prepare autoradiographs. Coverslips were acid-cleaned and dipped in Kodak NTB-2 emulsion and dried. The slides were apposed with the dipped coverslips and incubated in the dark at −20°C for 3 weeks to 4 months. The autoradiographs were developed in Kodak D-19, fixed in Kodak Rapid Fix without hardener, and counterstained with thionin.

The cytoarchitecture of the limbic thalamic nuclei was determined by inspection with brightfield optics. Darkfield illumination was then used to calculate the number of grains per 2,500 μm^2 field within a particular nucleus with a model 1000 Image Analysis system (Donsanto Corp., Natick, MA). Miscounts due to overlapping grains were visually corrected. Grain densities of three sections of total ligand binding and that for non-specific binding were counted and the mean was calculated for each nucleus in each animal. Non-specific binding was subtracted from total binding to determine specific binding. The mean ± S.E.M. specific binding was calculated for each thalamic nucleus. A one way analysis of variance was performed to analyze binding among nuclei. The F ratios with a $p < .0001$ are shown in Table 2. Multiple comparison protected t tests (Couch, '82) were performed to compare differences in binding in thalamic nuclei for each ligand. The computer program used for these analyses was produced by Dynamic Microsystems, Inc. (Silver Spring, MD).

RESULTS

Cytoarchitecture of limbic thalamic nuclei

Anterior thalamus. The anterior thalamic nuclei consist of the anterior dorsal (AD), anterior ventral (AV) and anterior medial (AM) nuclei. The AD nucleus is dorsal to AV and lateral to the stria medullaris and has two subdivisions as shown in Figure 1A. The parvicellular division (ADp) is composed of small and round or elongate neurons, while the magnocellular part (ADm) lies ventral to ADp and has large dark-staining neurons. The AV nucleus is also composed of two subdivisions. The magnocellular division (AVm) lies in the dorsomedial sector of AV and contains large, round neurons, while the parvicellular portion (AVp) contains smaller, round and elongated, pale-staining neu-

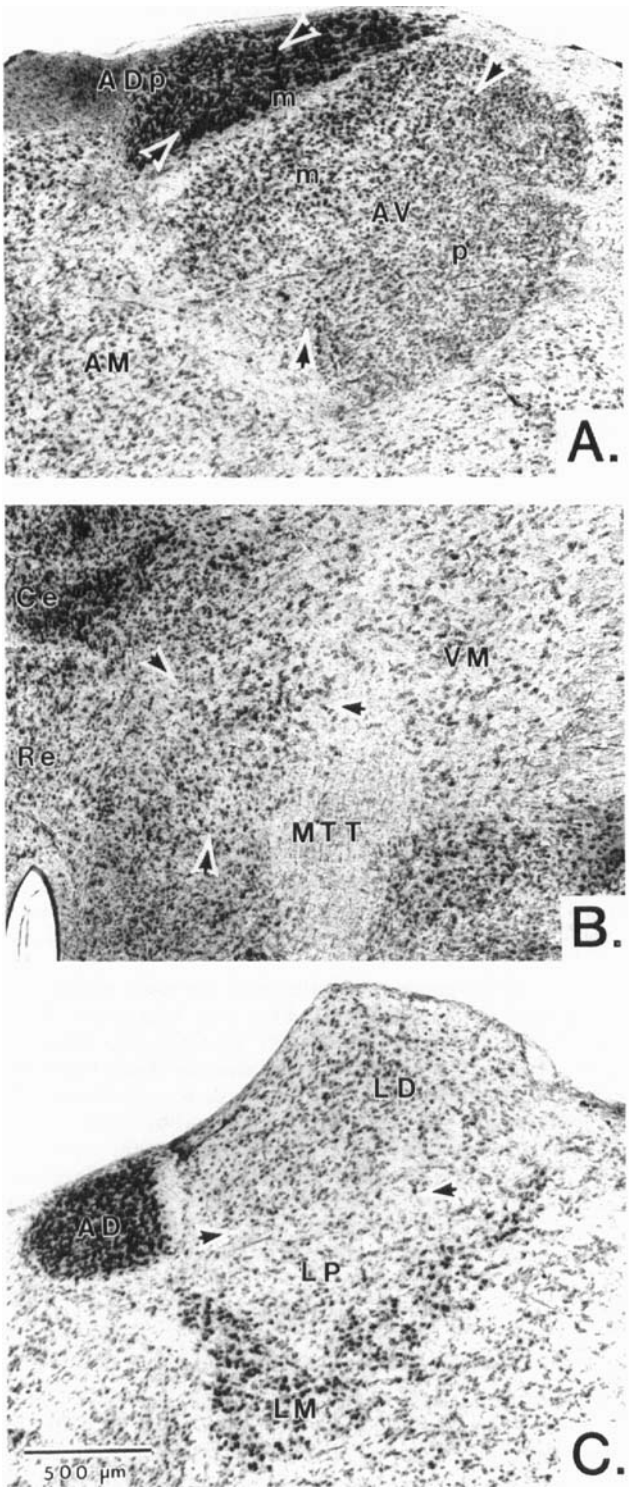

Fig. 1. Photomicrographs of coronal sections through the rabbit limbic thalamus in a celloidin-embedded and Nissl-stained case. **A:** Rostral level of limbic thalamus shows parvicellular and magnocellular divisions of AD and AV (marked by arrowheads). **B:** SM is marked by arrowheads and lies medial to MTT and lateral to Re and Ce. **C:** Caudal level of limbic thalamus demonstrating LD, LP, and LM. The arrowheads mark the border between LD and LP.

rons. The AVp is present in the anterior and middle parts of the rostrocaudal extent of AV, while AVm is larger at caudal levels. The AM nucleus lies medial to the AV nucleus and contains medium-sized, loosely arranged neurons.

Ventral thalamus. The cell groups in the ventral thalamus which project to limbic cortex include the ventral anterior (VA), ventral medial (VM), and submedial (SM) nuclei. The VA nucleus is ventral and lateral to the AV nucleus and contains neurons that are medium-sized, oval shaped, and loosely packed. The VM nucleus is medial to the ventral lateral nucleus, dorsolateral to the mamillothalamic tract, and contains loosely packed and large neurons as shown in Figure 1B. Rostral levels of the SM nucleus (delineated with arrowheads in Fig. 1B) are medial to the mamillothalamic tract and lateral to the reuniens and central nuclei. This nucleus contains round and medium-sized neurons that are packed more densely than are neurons in VM.

Lateral thalamus. The lateral thalamus in the rabbit is composed of three regions as shown in Figure 1C: lateral dorsal (LD), lateral posterior (LP) and lateral magnocellular (LM) nuclei. At the mid-rostrocaudal level of LD (Fig. 1C), this nucleus is lateral to AD and dorsal to LP. At rostral levels of LD, the LP nucleus is not present, while at caudal levels of LD, the AD nucleus is absent. The LD nucleus contains medium-sized and round neurons that are loosely packed. The LP nucleus lies ventral to LD and contains neurons that are smaller and lighter-staining than LD. The LM nucleus is a chevron-shaped group of neurons that underlies a rostral extension of LP and the most medial and lateral parts of LD. The LM nucleus contains the largest and most heavily stained neurons in the rabbit thalamus.

Midline and intralaminar thalamus. The midline thalamus includes of the rhomboid (Rh), central (Ce), and reuniens (Re) nuclei. The Rh nucleus lies medial and dorsal to AM and contains medium-sized neurons with a moderate packing density. The Ce nucleus is ventral to Rh and contains dark-staining, tightly packed neurons, as shown in Figure 1B. The Re nucleus lies between Ce and the third ventricle and contains small, lightly staining, loosely packed neurons. Finally, the central lateral (CL) and parafascicular (Pf) nuclei are intralaminar nuclei and are defined here according to Gerhard ('68). The CL nucleus is lateral to Ce and is usually ventral to AM and the mediodorsal nucleus. The CL nucleus contains light-staining, ovoid and loosely packed neurons. The Pf nucleus is pierced by the habenulo-interpeduncular tract and contains dark-staining, medium-sized neurons.

Retrograde labeling of thalamocortical projection neurons

Anterior cingulate injections. Ten injections were made into area 24b with 2–3 injections of different dyes in each case. One case was chosen as an example in which 3 dyes were injected into different rostrocaudal levels of area 24b. The injection of diamidino yellow into caudal area 24b is shown in Figure 2. Figure 3 shows these injection sites represented on a flattened medial surface on which the cytoarchitectural divisions of cingulate cortex are delineated and three representative sections are shown of retrogradely-labeled neurons in the thalamus. Following a rostral area 24b injection, the greatest number of labeled neurons occurred in AM, VA, and SM (Fig. 3A). The labeled neurons in AM were located dorsally within the nucleus.

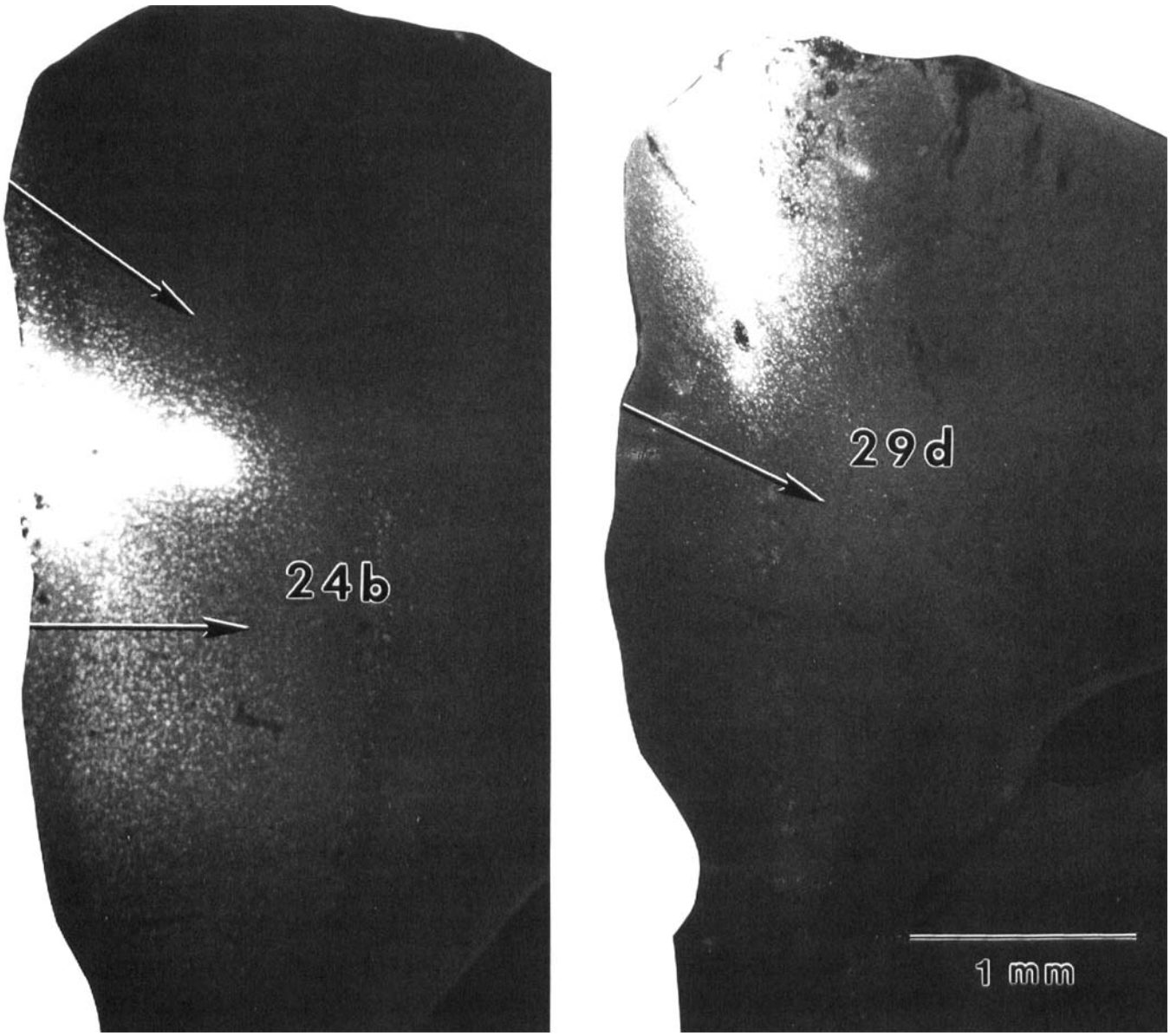

Fig. 2. Photomicrographs of diamidino yellow injections into caudal area 24b and rostral area 29d. The arrows in the first photograph delimit the border of area 24b, while the arrow in the second photograph shows the ventral border of area 29d.

The VA nucleus had labeled neurons that were located medially, while SM labeling occurred throughout this nucleus. There was also labeling in medial parts of the ventral lateral (VL) nucleus, throughout VM and in the parvicellular part of the medial dorsal (MDp) nucleus (Fig. 3B,C).

The caudal area 24b injection produced heavy labeling of neurons in AM, VA, and VL (Fig. 3A,B). There was a topographical organization of labeled neurons in AM, since caudal area 24b injections labeled neurons that were more ventral in AM than did rostral injections. Also, there was a topography within VA, VL, and MDp where caudal injections labeled neurons more laterally within these nuclei. Caudal area 24b injections also labeled neurons in LM, LP, LD, and CL, while rostral injections did not.

The Pf nucleus contained retrogradely labeled neurons following area 24b injections. These labeled neurons were located lateral to the habenulo-interpeduncular tract following both rostral and caudal area 24b injections. There was no apparent topography in Pf following injections into different parts of area 24b.

Posterior cingulate injections. Twenty-five injections were made into posterior cingulate cortex with 2–3 injections per case. A reconstruction of injection sites and labeled neurons for one case which received three injections in area 29d is shown in Figure 4. The anterior area 29d diamidino yellow injection is shown in Figure 2. Following a rostral diamidino yellow and a caudal fast blue injection into area 29d, most labeled neurons in the anterior thala-

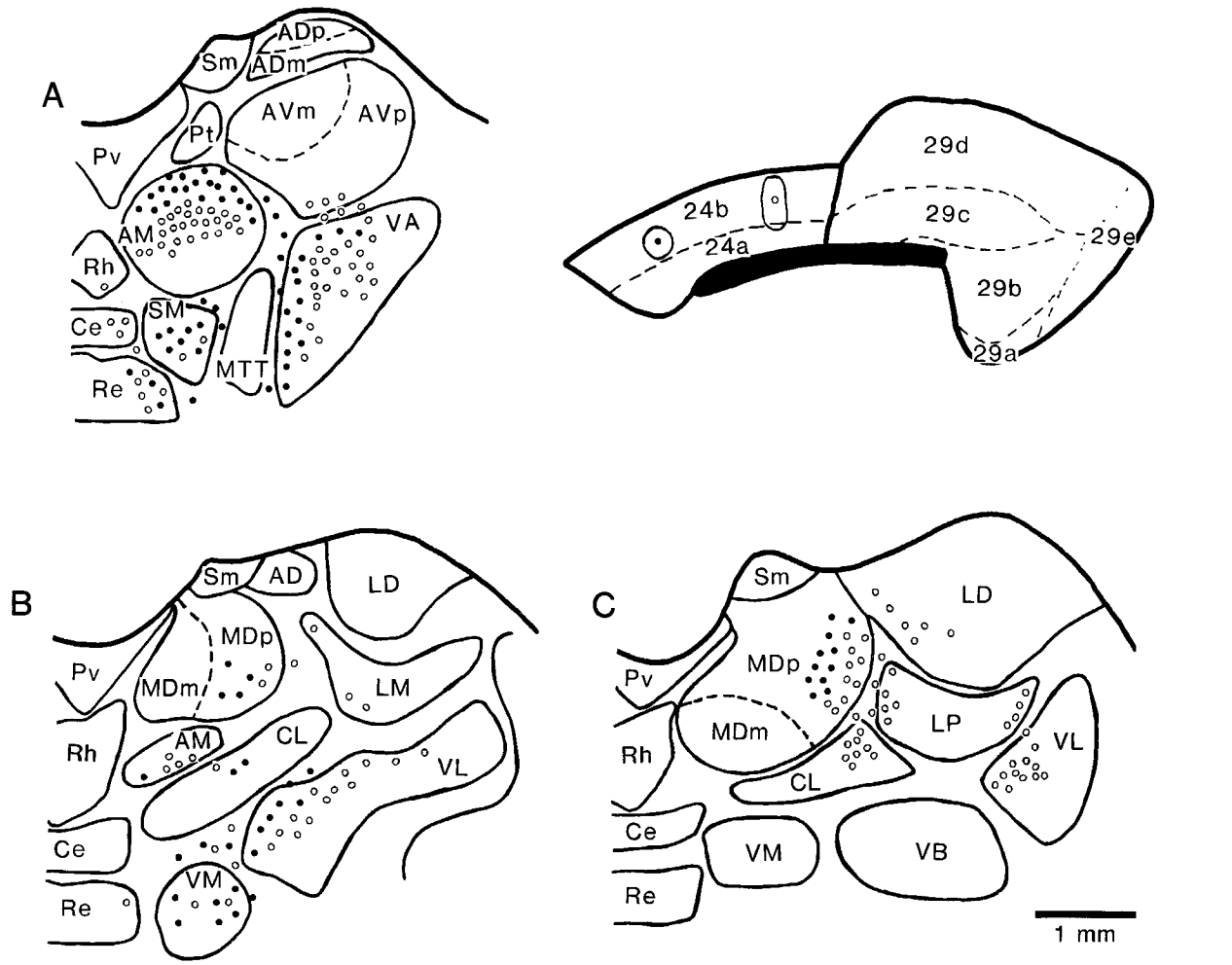

Fig. 3. Injections were made into two rostrocaudal levels of area 24b with rhodamine-labeled fluorescent latex microspheres (●) and diamidino yellow (○). Cytoarchitectural areas are displayed on a flattened medial surface above the corpus callosum (black) and positions of retrogradely labeled neurons in limbic thalamus are shown in transverse sections A–C. One dot represents four labeled neurons. Following a rostral area 24b injection, there was heavy labeling in dorsal AM, medial VA and SM, while a caudal area 24b injection produced heavy labeling in mid AM, VA, and VL.

mus were in AVp and AD (Fig. 4A); the intermediate injection of rhodamine-labeled fluorescent latex microspheres is not illustrated. Figure 5 is a photomicrograph showing labeled neurons in AVp, as well as Nissl-stained cells in a nearby section. The fiber bundles coursing through AVp are emphasized with asterisks in each section. The labeled neurons in AVp, but not AD, were topographically organized. Thus, the rostral diamidino yellow injection labeled neurons medially in AVp, while the labeled neurons following the caudal fast blue injection were more lateral. The injection of rhodamine-labeled fluorescent latex microspheres intermediate between the rostral and caudal area 29d injections labeled neurons in AVp between the diamidino and fast blue labeled neurons (not illustrated). The AD nucleus contained neurons double-labeled with diamidino yellow and microspheres, while AVp did not contain double-labeled neurons. The caudal area 29d injection also labeled neurons in VA. In caudal levels of the thalamus (Fig. 4B,C), area 29d injections labeled neurons in LM, LP, MDp, and VL. Finally, rostral area 29d injections labeled neurons in LP more medially than did injections into caudal area 29d (Fig. 4C).

Figure 6 represents a case with area 29c and area 29b injections. Following the caudal area 29c rhodamine-labeled fluorescent latex microsphere injection and the 29b diamidino yellow injection, most labeled neurons in anterior thalamus were in AD and AV. Both parvicellular and magnocellular divisions of AD contained labeled cells and there was no apparent segregation within this nucleus. Labeled neurons in AV also occurred in both divisions. Although there was no segregation of labeled neurons in either division of AV, labeled neurons with both dyes were located laterally within AV. There was less labeling in AM following both injections in contrast to that produced by injections into anterior cingulate cortex. In caudal parts of the thalamus, area 29c and 29b injections labeled neurons in LM, LP and LD, with LP and LD containing the highest density of labeled neurons (Fig. 6B,C). There was minimal labeling in VL following the caudal area 29c injection.

Table 1 presents the percentage of labeled cells in each nucleus as well as the total number of labeled neurons for each injection site presented in Figures 3, 4, and 6. A qualitative assessment of anterior to posterior changes in the density of labeled neurons in each nucleus following

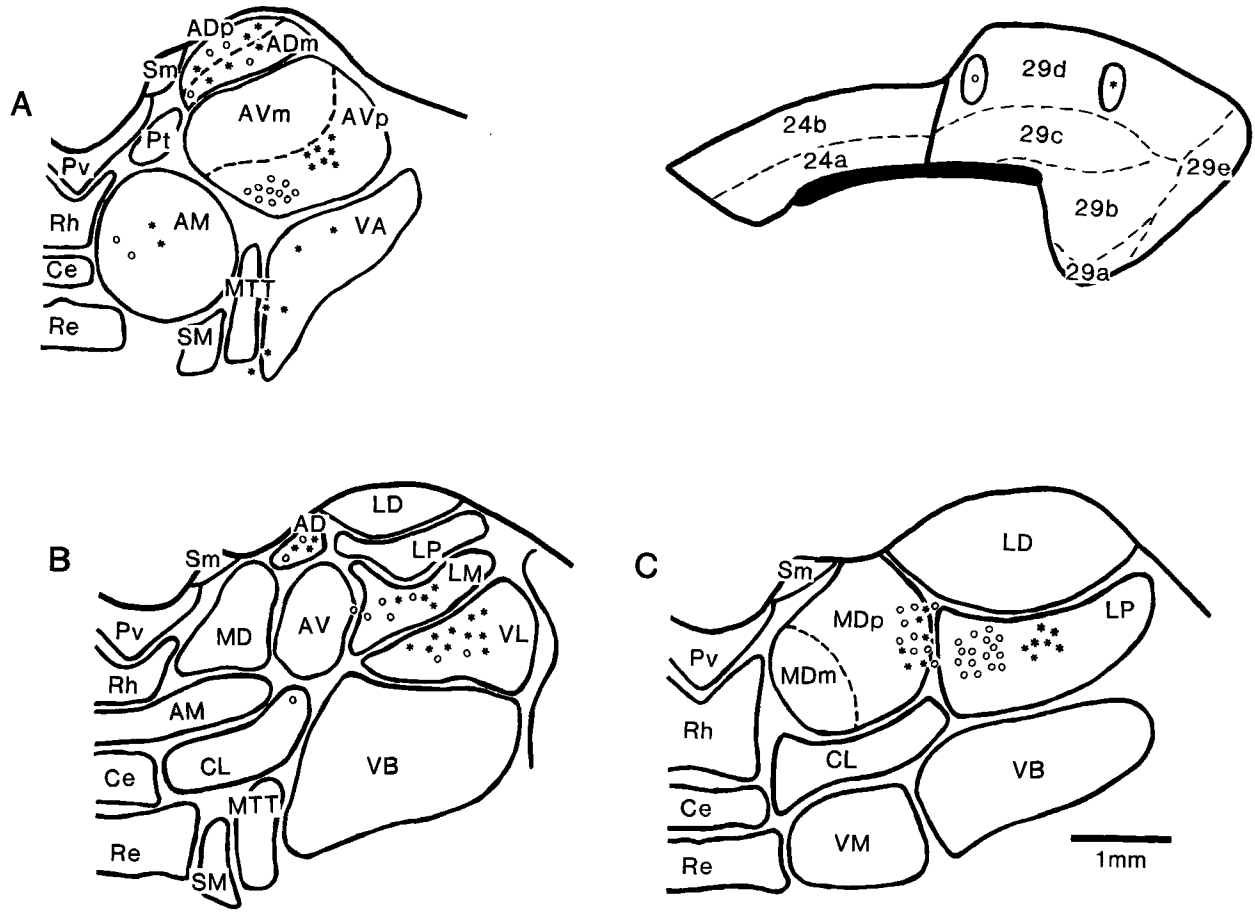

Fig. 4. Injections of diamidino yellow (○) and fast blue (*) were made into area 29d and labeled neurons in limbic thalamus are shown in transverse sections **A–C.** Area 29d injections labeled neurons in AD and AVp, with those in AVp topographically organized.

progressively more caudal injections is shown in the last column under "Trend." Cases with injections into anterior cingulate cortex had highest labeling in AM, VA, SM, and MDp, and labeling in these nuclei decreased with injections into progressively more caudal cingulate cortex. Labeling of neurons in Re, VM, and CL was limited but also showed a decrease in density with more caudal injections. Neurons labeled in the ADp, ADm, AVm, LM, and LD nuclei were most prominent following injections into caudal cingulate cortex. This labeling increased with injections into progressively more caudal levels of cingulate cortex.

There were very different patterns of thalamic neuron labeling following injections into different cytoarchitectural divisions of posterior cingulate cortex. As shown in Table 1, about 40% of the neurons labeled in the thalamus following area 29d injections were in LP. In contrast, less than half this percentage of neurons were labeled following the area 29c injection. In this latter case, 12–19% of the labeled neurons were in each of the ADm, AVp, and LD nuclei. In the area 29b injection, 10.9% of the labeled neurons were in LP, while 20.3% were in AVm and 14.2% were in ADm. Although there were relatively few labeled neurons in VA and VL following the rostral area 29d injection, there was elevated labeling in these nuclei after the caudal area 29d injection. Since labeling in these nuclei was also high following injections into the middle anteroposterior level of area 24b, it appears that there were two foci in dorsal cingulate cortex which receive inputs from these nuclei. Finally, it is of interest that the total number of labeled cells were generally higher following rostral cingulate cortex injections (642–1,125 labeled neurons) than following injections into caudal cingulate cortex (395–596 labeled neurons). These injections did not appear to differ in size.

Ligand binding

Muscarinic receptors. Table 2 is a summary of the specific binding for 18 rabbits for the ligands studied. Each division of the anterior nuclei and the LM, LD, SM, and Pf nuclei were analyzed. Specific pirenzepine binding was highest in the AVm, AM, and LD nuclei and there was no difference in the binding in these nuclei. There were significant differences in pirenzepine binding between AM and the following nuclei: ADp, ADm, AVp, LM, SM, and Pf. The lowest density of pirenzepine binding was observed in the ADm and Pf nuclei. In contrast to the very high pirenzepine binding in AM, this nucleus had one of the lowest densities of OXO-M/PZ binding. The highest OXO-M/PZ binding in the limbic thalamus was in ADp, while that in ADm was about half of that density. Figure 7B is a

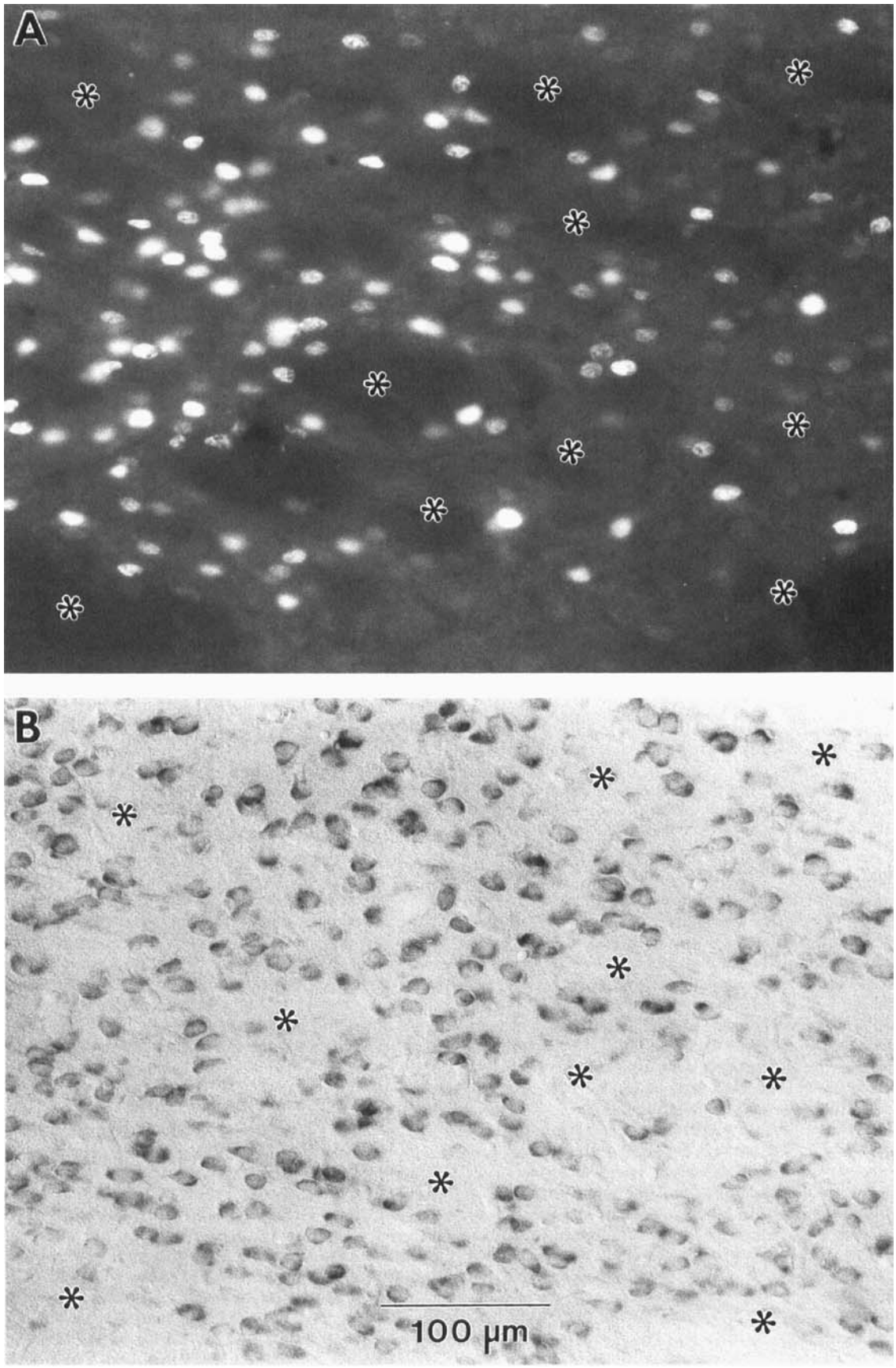

Fig. 5. **A:** Photomicrograph of labeled neurons in AVp, following a diamidino yellow injection into rostral area 29d. **B:** Photomicrograph of Nissl-stained AVp within 250 μm of that in A. Fiber bundles are characteristic of AVp and are marked by asterisks. Also note the small, elongate and round pale-staining neurons that are characteristic of AVp.

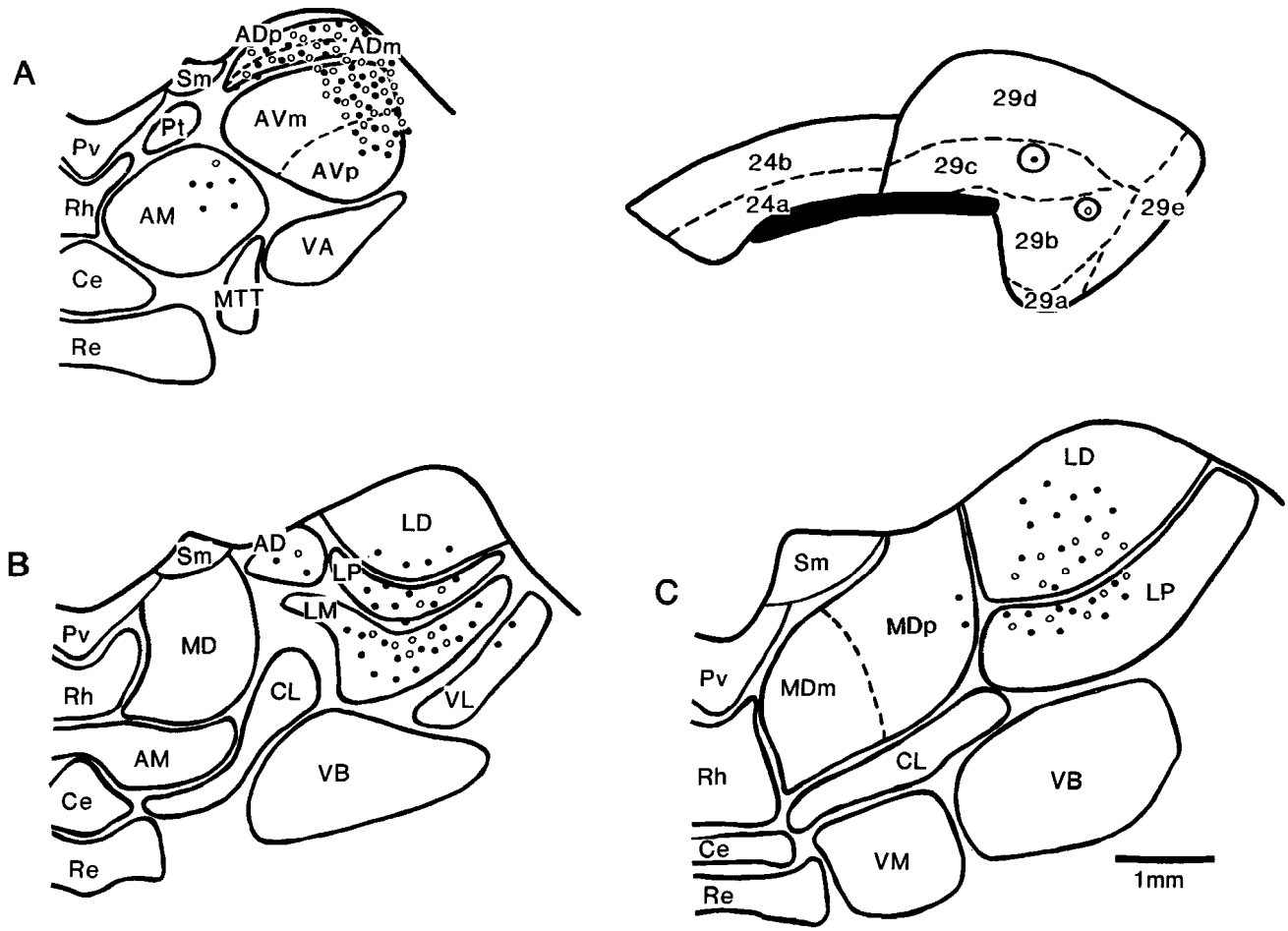

Fig. 6. Injections of rhodamine-labeled fluorescent latex microspheres (●) and diamidino yellow (○) were made into areas 29c and 29b, respectively, and labeled neurons in the thalamus are shown in sections **A–C.** Area 29c and 29b injections labeled neurons in AD, AV, and the lateral nuclei, with heaviest labeling in AVm.

TABLE 1. Proportion of Total Labeled Neurons in Each Limbic Thalamic Nucleus

Nuclei	Rostral 24b	Caudal 24b	Rostral 29d	Caudal 29d	Caudal 29c	Caudal 29b	Trend A → P
ADp	—	—	5.9	6.4	7.2	12.7	↑
ADm	—	—	8.4	7.2	11.7	14.2	↑
AVp	—	1.4	13.8	8.0	12.1	7.1	—
AVm	—	—	—	—	10.7	20.3	↑
AM	26.5	19.2	5.7	1.8	3.5	1.0	↓
Rh	—	0.5	—	—	—	—	—
Re	5.1	4.6	—	0.6	—	—	↓
VA	23.1	17.7	0.5	5.8	—	—	↓
VL	4.8	13.6	2.5	11.0	3.9	—	—
VM	5.5	0.9	—	—	—	—	↓
VB	—	—	0.5	0.2	—	—	—
Ce	—	2.2	1.7	1.0	—	1.3	—
CL	1.4	3.6	1.2	0.2	—	—	↓
SM	12.6	1.4	—	0.4	—	—	↓
LM	—	1.2	4.4	4.4	10.1	13.7	↑
LD	—	2.1	—	3.8	19.0	19.0	↑
LP	—	6.8	41.5	38.8	19.5	10.9	—
MDp	19.5	22.4	13.8	10.2	2.3	—	↓
Pf	1.6	2.3	—	—	—	—	—
Total cells	642	1,125	405	498	596	395	↓

photomicrograph of OXO-M/PZ binding in these subnuclei, and shows the relatively high binding in ADp in comparison to that in ADm.

TABLE 2. Specific Binding (Grains ± S.E.M./2,500 μm²)

	Pirenzepine	OXO-M/PZ	Muscimol	DAGO	DPDPE
ADp	147 ± 8[1]	245 ± 13[2]	240 ± 7[1]	97 ± 4[1]	142 ± 6[2]
ADm	87 ± 6[1]	128 ± 9[1]	184 ± 9[1]	45 ± 2[1]	71 ± 4[1]
AVp	128 ± 7[1]	124 ± 8[1]	309 ± 9[2]	81 ± 6[1]	79 ± 4[1]
AVm	184 ± 10[2]	75 ± 5[1]	312 ± 11[2]	160 ± 8[2]	92 ± 4[1]
AM	214 ± 14[2]	56 ± 6[1]	203 ± 7[1]	127 ± 5[1]	74 ± 4[1]
LM	119 ± 6[1]	31 ± 5[1]	128 ± 6[1]	72 ± 4[1]	36 ± 2[1]
LD	190 ± 9[2]	94 ± 7[1]	262 ± 7[1]	149 ± 6[2]	63 ± 4[1]
SM	116 ± 6[1]	59 ± 3[1]	76 ± 4[1]	118 ± 5[1]	78 ± 5[1]
Pf	87 ± 6[1]	79 ± 5[1]	55 ± 6[1]	140 ± 10[2]	76 ± 5[1]
F-Ratio*	30	74	149	42	41

*All ANOVA F ratios have a $p < .0001$.
[1]Values significantly different from the highest value at $p < .01$.
[2]Highest densities of specific binding for each ligand.

GABA receptors. Specific muscimol binding was highest in the AV nucleus in both AVp and AVm. Muscimol binding in these subnuclei was not significantly different. The AM, AD, LD, LM, SM, and Pf nuclei all had lower densities of muscimol binding.

Opioid receptors. Specific DAGO binding distinguished between the divisions of AV. The highest density of DAGO binding in limbic thalamus was in AVm, while AVp had only half as much DAGO binding. Binding of DPDPE did not distinguish between the subdivisions of AV.

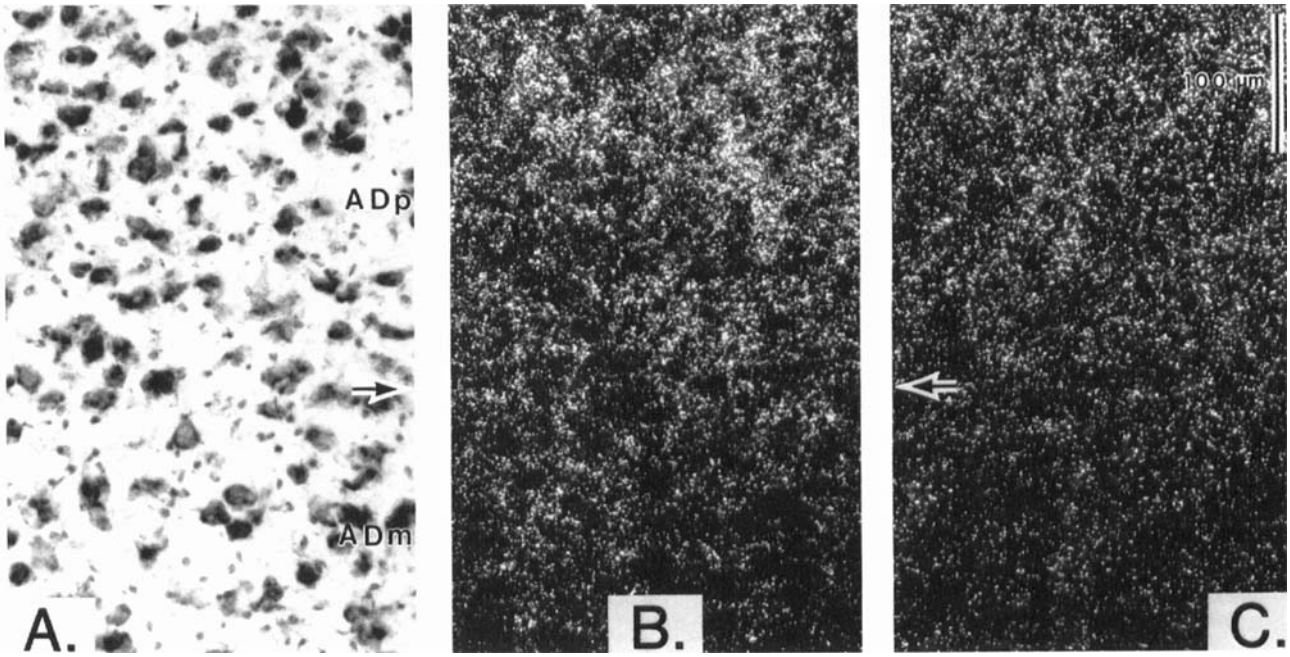

Fig. 7. **A:** Photomicrograph of Nissl-stained, cryostat section, demonstrating divisions of AD. **B:** The binding of OXO-M/PZ in ADp is twice as dense as that in ADm. **C:** The binding of DPDPE is also high in ADp and low in ADm. The border between ADp and ADm is marked by arrows.

The binding of both opioid compounds was significantly different for each of the subdivisions of AD. The ADp nucleus had high DAGO and DPDPE binding; however, ADm had only one-half this binding. The photomicrograph in Figure 7C demonstrates the differences in DPDPE binding in ADp and ADm, with that in ADp being very high. The striking differences in OXO-M/PZ and DPDPE binding in ADp and ADm confirms cytoarchitectural observations that these are distinct subnuclei. Finally, DAGO binding was high in AVm, LD, and Pf, and the binding of DPDPE was homogeneous throughout the limbic thalamus, except for the high binding previously noted in ADp.

DISCUSSION

A large number of thalamic nuclei project to cingulate cortex and are here referred to as the limbic thalamus. The role of these nuclei in cortical function is likely more complex than that of the sensory and motor thalamic nuclei in that limbic nuclei may participate in affective responses to noxious stimuli, learning and memory. Since the rabbit is being increasingly used in functional studies of the nervous system, more information is needed about the structure and connections of its limbic thalamus. The present study detailed the unique cytoarchitectural features of the rabbit limbic thalamic nuclei, their projections to cingulate cortex and the distribution of transmitter receptors that have differential binding in particular subnuclei and so differentially modulate parts of limbic thalamocortical circuitry.

The division of the AD nucleus into parvicellular and magnocellular components appears to be unique to the rabbit brain. These cytoarchitectural divisions of AD have very different patterns in transmitter receptor binding, although each has broad projections throughout area 29. The AD nucleus itself is unique among the limbic thalamic nuclei because it receives little or no cingulate cortical (Domesick, '72; Vogt, '85) or cholinergic (Levey et al., '87) inputs, while its main input is from the mamillary bodies (Cruce, '75; Veazey et al., '82; Seki and Zyo, '84). These connections likely determine the form of neuronal activity in AD during the acquisition of avoidance learning in rabbits. Thus, neurons in AD produce massive excitatory responses to conditional stimuli during the earliest stages of avoidance training. These excitatory responses subside and become discriminative (i.e., greater excitatory responses to the positive than the negative conditional stimulus) when the rabbit attains criterion avoidance responding (Gabriel et al., '91). Section of the mamillothalamic tract reduces the excitatory responses in AD, while removal of cingulate cortex increases excitatory responses in AV (Gabriel et al., '88). Thus, a lack of inhibitory cingulate cortical control and a dominant excitatory projection from the mamillary bodies likely result in the hyperexcitability of neurons in the AD nucleus during discriminative avoidance learning.

The midline and intralaminar thalamic nuclei are part of the limbic thalamus and contain neurons that respond to noxious stimuli (Casey, '66; Dong et al., '78; Peschanski et al., '81; Ma et al., '88; Miletic and Coffield, '89). The SM and Pf nuclei are among those nuclei that receive direct projections from the spinal cord, including neurons in lamina I (Craig and Burton, '81, '85; Dado and Giesler, '90), and project in turn to cingulate cortex in the cat (Robertson and Kaitz, '81; Craig et al., '82; Musil and Olson, '88) and monkey (Vogt et al., '79, '87). Injections of fluorescent dyes into rostral area 24b of the rabbit in the present study labeled neurons in SM and Pf. In light of recent findings that neurons in rostral area 24b respond to noxious mechanical and thermal stimuli and the block of these responses by medial thalamic injections of lidocaine (Sikes and Vogt,

'91), it is likely that SM and Pf projections to cingulate cortex contribute to responses to noxious stimuli in anterior cingulate cortex. Furthermore, SM has enkephalin-immunoreactive axons (Miletic and Coffield, '88) and the present study shows that SM and Pf have moderate densities of mu and delta opioid receptors. Therefore, neuronal activity in SM and Pf likely contributes to nociceptive neuronal activity in limbic cortex and is modulated by enkephalinergic connections.

Since all previous opioid receptor binding studies have been done with film autoradiography, no studies are available which localize these receptors to subnuclei within the limbic thalamus. The present study employed coverslip autoradiography, and so a number of new issues can be raised about the distribution of opioid receptors. First, the most striking observation of the present study was that DPDPE binding was highest in ADp. The dichotomy of high DPDPE binding in ADp and low binding in ADm confirms cytoarchitectural observations of the present study that AD has two subdivisions. In a previous study of delta opioid ligand binding in rat (McLean et al., '86), there was almost no such binding in AD. One interpretation of these findings is that the rat does not have an equivalent to the rabbit ADp nucleus. Second, McLean et al. ('86) observed high mu opioid binding in AM and LD as was true for the present study. However, as shown in Table 2, highest densities of DAGO binding were in AVm. The earlier finding of sparse mu binding in AV could have been due to differences in ligand specificity. Furthermore, enkephalin-immunoreactive axons have been noted in AV (Sar et al., '78; Finley et al., '81) and immunoreactive neurons in the mamillary bodies. Since the mammillary bodies project to AV, it is possible that enkephalinergic mamillothalamic projections modulate the activity of AD, AV, and AM neurons via mu opioid receptors.

The AVp nucleus has one of the highest levels of choline acetyltransferase activity in the thalamus (Levey et al., '87) and this input arises from neurons in the lateral dorsal tegmental, cuneiform and pedunculopontine nuclei (Hoover and Baisden, '80; Sofroniew et al., '85; Satoh and Fibiger, '86). The present analysis shows that AVp projects mainly to areas 29c and 29d and less to area 29b, while AVm projects more heavily to caudal area 29c and area 29b. Therefore, the influence of cholinergic activity in the thalamus is principally on neurons which project to mid-levels of cingulate cortex, not caudal and ventral cingulate cortical areas. It was the AVp and mid-levels of cingulate cortex which had increased binding of OXO-M/PZ in rabbits trained to first significant and criterion stages of discriminative avoidance learning (Vogt et al., '91). Thus, it is possible that cholinergic connections, particularly to AVp, play a role in elevating muscarinic binding during the acquisition of this task.

The distribution of muscarinic ligand binding in limbic thalamus reported in this study raises a number of issues about the cellular localization of muscarinic receptors. First, pirenzepine binding is high in AM, AVm, and LD. Although pirenzepine binds to m1, m3 and m4 receptors (Buckley et al., '89), m3 but not m1 and m4 receptors are expressed by rat thalamic neurons (Buckley et al., '88). Therefore, pirenzepine binding is likely to m3 receptors throughout limbic thalamus. Second, OXO-M/PZ binding is a protocol which has enhanced binding to m2 receptors (Vogt and Burns, '88; Vogt et al., '92). It is striking that highest OXO-M/PZ binding occurred in ADp which receives no cholinergic afferents. Although in situ studies of mRNA for the m2 receptor have failed to show expression of this receptor by AD neurons (Buckley et al., '88), experimental ligand binding studies suggest that AD neurons transport these receptors to their axon terminals in cingulate cortex. Van Groen and Wyss (personal communication) have observed AD projections to layer III of area 29c, and Vogt et al. ('92) have demonstrated a massive reduction in OXO-M/PZ binding in layer III following thalamic lesions. Thus, most OXO-M/PZ binding in ADp is likely associated with newly synthesized m2 receptors which are destined for transport to cingulate cortex. Third, OXO-M/PZ binding in AVp was at moderate levels and may reflect binding to m2 receptors on two cellular elements in this nucleus; autoreceptors on cholinergic afferents from the brainstem and "presynaptic" m2 receptors which are synthesized in AV (Buckley et al., '88) and transported to cingulate cortex (Vogt et al., '92).

The rat anterior thalamus does not contain GABAergic neurons; however, the AV nucleus shows immunoreactivity for the enzyme GAD (Tappaz et al., '76; Mugnaini and Oertel, '85). The highest levels of muscimol binding in the present study of the rabbit occurred in AV, with significant differences in binding between AV and the other limbic nuclei. These data support the findings of Palacios et al. ('81) who demonstrated that AV contained a high number of high-affinity GABA receptors. Therefore, GABAergic control differs among the limbic thalamic nuclei.

The ventral anterior and ventral lateral thalamic nuclei project to cingulate cortex in the depths of the cingulate sulcus of the monkey brain (Vogt et al., '87; Holsapple and Strick, '89). The present study shows that VA has a major projection to dorsal cingulate area 24b and also has a small projection to area 29d in the rabbit. The VL nucleus also has moderate projections to areas 24b and 29d. There are four reasons for suggesting that parts of cingulate cortex are involved in motor functions. First, on the basis of lipofuscin content of neurons, Braak ('76) proposed that cortex in the depths of the human cingulate sulcus may contain a motor area. Second, the VA and VL nuclei have been implicated in motor functions and receive inputs from different motor systems. Thus, the VA nucleus receives projections from the globus pallidus and the substantia nigra (Strick, '85; Ilinsky et al., '85; Ilinsky and Kultas-Ilinsky, '87) and VL receives input from the cerebellum (Kalil, '81; Schell and Strick, '84). Third, cortex in the depths of the monkey cingulate sulcus and area 24b in the rat have projections to the spinal cord (Biber et al., '78; Miller, '87; Hutchins et al., '88; Dum and Strick, '91). Fourth, Shima et al. ('91) demonstrated two movement-related foci in cingulate areas 24c and 23c in the monkey during signal-triggered and self-paced forelimb movements. Anterior cingulate cortex contained more self-paced neurons and neurons that discharged 500 msec or more before movement than did posterior cingulate cortex. The hypothesis was proposed by Shima et al. ('91) that the anterior cingulate motor area mediates the internal drive for movements. In conclusion, although the rabbit does not have a cingulate sulcus, dorsal cingulate area 24b receives a large input from VA and a smaller input from VL, suggesting that area 24b may contain a motor area in the rabbit. Furthermore, based on VA/VL projections, there may be two discrete cingulate motor regions in the rabbit. One may

be located at a mid-rostrocaudal level of area 24b and one in caudal area 29d.

The rabbit has become an important species for neurobiological studies because of its highly differentiated posterior cingulate cortex. The present study of the rabbit limbic thalamus shows that these nuclei are also highly differentiated, have topographically organized connections to cingulate cortex, and that afferent transmitter systems differentially regulate these thalamocortical projection neurons. These limbic nuclei likely play an important role in responses to noxious stimuli and learning, and "limbic" parts of VA and VL may contribute to motor functions in cingulate cortex.

ACKNOWLEDGMENTS

This research was supported by NIH-NINDS grant NS18745 and NIH-NIDA grant P50 DA06634.

LITERATURE CITED

Biber, M.P., L.W. Kneisley, and J.H. LaVail (1978) Cortical neurons projecting to the cervical and lumbar enlargements of the spinal cord in young and adult rhesus monkeys. Exp. Neurol. *59:*492–508.

Braak, H. (1976) A primitive gigantopyramidal field buried in the depth of the cingulate sulcus of the human brain. Brain Res. *109:*219–233.

Buchanan, S.L., D.A. Powell, and R.H. Thompson (1989) Prefrontal projections to the medial nuclei of the dorsal thalamus in the rabbit. Neurosci. Lett. *106:*55–59.

Buckley, N.J., T.I. Bonner, and M.R. Brann (1988) Localization of a family of muscarinic receptor mRNAs in rat brain. J. Neurosci. *8:*4646–4652.

Buckley, N.J., T.I. Bonner, C.M. Buckley, and M.R. Brann (1989) Antagonist binding properties in five cloned muscarinic receptors expressed in CHO-K1 cells. Mol. Pharmacol. *35:*469–476.

Casey, K.L. (1966) Unit analysis of nociceptive mechanisms in the thalamus of the awake squirrel monkey. J. Neurophysiol. *29:*727–750.

Couch, J.V. (1982) Fundamentals of Statistics for the Behavioral Sciences. New York: St Martin's Press, pp. 266–270.

Craig, A.D., and H. Burton (1981) Spinal and medullary lamina I projection to nucleus submedius in medial thalamus: A possible pain center. J. Neurophysiol. *45:*443–466.

Craig, A.D., and H. Burton (1985) The distribution and topographical organization in the thalamus of anterogradely-transported horseradish peroxidase after spinal injections in cat and raccoon. Exp. Brain Res. *58:*227–254.

Craig, A.D., S.J. Wiegand, and J.L. Price (1982) The thalamo-cortical projection of the nucleus submedius in the cat. J. Comp. Neurol. *206:*28–48.

Cruce, J.A.F. (1975) An autoradiographic study of the projections of the mammillothalamic tract in the rat. Brain Res. *85:*211–219.

Dado, R.J., and G.J. Giesler, Jr. (1990) Afferent input to nucleus submedius in rats: Retrograde labeling of neurons in the spinal cord and caudal medulla. J. Neurosci. *10:*2672–2686.

Domesick, V.B. (1972) Thalamic relationships of the medial cortex in the rat. Brain Behav. Evol. *6:*457–483.

Dong, W.K., H. Ryu, and I.H. Wagman (1978) Nociceptive responses of neurons in medial thalamus and their relationship to spinothalamic pathways. J. Neurophysiol. *41:*1592–1613.

Dum, R.P., and P.L. Strick (1991) The origin of corticospinal projections from the premotor areas in the frontal lobe. J. Neurosci. *11:*667–689.

Finley, J.C.W., J.L. Maderdrut, and P. Petrusz (1981) The immunocytochemical localization of enkephalin in the central nervous system of the rat. J. Comp. Neurol. *198:*541–565.

Gabriel, M., Y. Kubota, and J. Shenker (1988) Limbic circuit interactions during learning. In H. Markowitsch (ed): Information Processing by the Brain. Toronto: Hans Huber Publishers, pp. 39–63.

Gabriel, M., B.A. Vogt, Y. Kubota, A. Poremba, and E. Kang (1991) Training-stage related neuronal plasticity in limbic thalamus and cingulate cortex during learning: A key to mnemonic retrieval. Behav. Brain Res. *46:*175–185.

Gerhard, L. (1968) Atlas des Mittel-und Zwischenhirns des Kaninchens. Berlin: Springer-Verlag.

Herkenham, M. (1978) The connections of the nucleus reuniens thalami: Evidence for a direct thalamo-hippocampal pathway in the rat. J. Comp. Neurol. *177:*589–610.

Holsapple, J.W., and P.L. Strick (1989) Premotor areas on the medial wall of the hemisphere: Input from ventrolateral thalamus. Soc. Neurosci. Abstr. *15:*282.

Hoover, D.B., and R.H. Baisden (1980) Localization of putative cholinergic neurons innervating the anteroventral thalamus. Brain Res. Bull. *5:*519–524.

Horikawa, K., N. Kinjo, L.C. Stanley, and E.W. Powell (1988) Topographic organization and collateralization of the projections of the anterior and laterodorsal thalamic nuclei to cingulate areas 24 and 29 in the rat. Neurosci. Res. *6:*31–44.

Hutchins, K.D., A.M. Martino, and P.L. Strick (1988) Corticospinal projections from the medial wall of the hemisphere. Exp. Brain Res. *71:*667–672.

Ilinsky, I.A., and K. Kultas-Ilinsky (1987) Sagittal cytoarchitectonic maps of the Macaca mulatta thalamus with a revised nomenclature of the motor-related nuclei validated by observations on their connectivity. J. Comp. Neurol. *262:*331–364.

Ilinsky, I.A., M.L. Jouandet, and P.S. Goldman-Rakic (1985) Organization of the nigrothalamocortical system in the rhesus monkey. J. Comp. Neurol. *236:*315–330.

Jones, E.G., and R.Y. Leavitt (1974) Retrograde axonal transport and the demonstration of nonspecific projections to the cerebral cortex and striatum from thalamic intralaminar nuclei in the rat, cat and monkey. J. Comp. Neurol. *154:*349–378.

Kaelber, W.M., C.L. Mitchell, A.J. Yarmat, A.K. Afifi, and S.A. Lorens (1975) Centrum medianum-parafascicularis lesions and reactivity to noxious and non-noxious stimuli. Exp. Neurol. *46:*282–290.

Kalil, K. (1981) Projections of the cerebellar and dorsal column nuclei upon the thalamus of the rhesus monkey. J. Comp. Neurol. *195:*25–50.

Katz, L.L., A. Burkhalter, and W.J. Breyer (1984) Fluorescent latex microspheres as a retrograde neuronal marker for in vivo and in vitro studies of visual cortex. Nature *310:*498–500.

Keizer, K., H.G.J.M. Kuypers, A.M. Huisman, and O. Dann (1983) Diamidino yellow dihydrochloride (DY 2HCl); A new fluorescent retrograde neuronal tracer which migrates only very slowly out of the cell. Exp. Brain Res. *51:*179–191.

Kobayashi, R.M., M. Palkovits, R.E. Hruska, R. Rothschild, and H.I. Yamamura (1978) Regional distribution of muscarinic cholinergic receptors in rat brain. Brain Res. *154:*13–23.

Levey, A.I., A.E. Hallanger, and B.H. Wainer (1987) Choline acetyltransferase immunoreactivity in the rat thalamus. J. Comp. Neurol. *257:*317–332.

Ma, W., M. Peschanski, and P.T. Ohara (1988) Fine structure of the dorsal part of the nucleus submedius of the rat thalamus: An anatomical study with reference to possible pain pathways. Neuroscience *26:*147–159.

Macchi, G., M. Bentivoglio, C. D'Atena, P. Rossini, and E. Tempesta (1977) The cortical projections of the thalamic intralaminar nuclei restudied by means of the HRP retrograde axonal transport. Neurosci. Lett. *4:*121–126.

Mansour, A., H. Khachaturian, M.E. Lewis, H. Akil, and S.J. Watson (1987) Autoradiographic differentiation of mu, delta, and kappa opioid receptors in the rat forebrain and midbrain. J. Neurosci. *7:*2445–2464.

Matsuoka, H. (1986) Topographic arrangement of the projection from the anterior thalamic nuclei to the cingulate cortex in the cat. Neurosci. Res. *4:*62–66.

McLean, S., R.B. Rothman, and M. Herkenham (1986) Autoradiographic localization of μ- and δ- opioid receptors in the forebrain of the rat. Brain Res. *378:*49–60.

Miletic, V., and J.A. Coffield (1988) Enkephalin-like immunoreactivity in the nucleus submedius of the cat and rat thalamus. Somatosens. Res. *5:*325–334.

Miletic, V., and J.A. Coffield (1989) Responses of neurons in the rat nucleus submedius to noxious and innocuous mechanical cutaneous stimulation. Somatosens. and Motor Res. *6:*567–587.

Miller, M.W. (1987) The origin of corticospinal projection neurons in rat. Exp. Brain Res. *67:*339–351.

Minciacchi, D., M. Bentivoglio, M. Molinari, K. Kultas-Ilinsky, I.A. Ilinsky, and G. Macchi (1986) Multiple cortical targets of one thalamic nucleus: The projections of the ventral medial nucleus in the cat studied with retrograde tracers. J. Comp. Neurol. *252:*106–129.

Moskowitz, A.S., and R.R. Goodman (1984) Light microscopic autoradiographic localization of μ and δ opioid binding sites in the mouse central nervous system. J. Neurosci. *4:*1331–1342.

Mugnaini, E., and W.H. Oertel (1985) An atlas of the distribution of GABAergic neurons and terminals in the rat CNS as revealed by GAD immunohistochemistry. In A. Bjorklund and T. Hokfelt (eds): Handbook of Chemical Neuroanatomy, Vol. 4. New York: Elsevier Science Publishing, pp. 436–608.

Musil, S.Y., and C.R. Olson (1988) Organization of cortical and subcortical projections to anterior cingulate cortex in the cat. J. Comp. Neurol. *272:*203–218.

Palacios, J.M., J.K. Wamsley, and M.J. Kuhar (1981) High affinity receptors-autoradiographic localization. Brain Res. *222:*285–307.

Peschanski, M., G. Guilbaud, and M. Gautron (1981) Posterior intralaminar region in rat: Neuronal responses to noxious and nonnoxious cutaneous stimuli. Exp. Neurol. *72:*226–238.

Robertson, R.T., and S.S. Kaitz (1981) Thalamic connections with limbic cortex. I. Thalamocortical projections. J. Comp. Neurol. *195:*501–525.

Rose, J.E., and C.N. Woolsey (1948) Structure and relations of limbic cortex and anterior thalamic nuclei in rabbit and cat. J. Comp. Neurol. *89:*279–340.

Rotter, A., N.J.M. Birdsall, A.S.V. Burgen, P.M. Field, E.C. Hulme, and G. Raisman (1979) Muscarinic receptors in the central nervous system of the rat. I. Technique for autoradiographic localization of the binding of [^{3}H]propylbenzilylcholine mustard and its distribution in the forebrain. Brain Res. Rev. *1:*141–165.

Royce, G.J., and R.J. Mourey (1985) Efferent connections of the centromedian and parafascicular thalamic nuclei: An autoradiographic investigation in the cat. J. Comp. Neurol. *235:*277–300.

Royce, G.J., S. Bromley, C. Gracco, and R.M. Beckstead (1989) Thalamocortical connections of the rostral intralaminar nuclei: An autoradiographic analysis in the cat. J. Comp. Neurol. *288:*555–582.

Sar, M., W.E. Stumpf, R.J. Miller, K.J. Chang, and P. Cuatrecasas (1978) Immunohistochemical localization of enkephalin in rat brain and spinal cord. J. Comp. Neurol. *182:*17–38.

Satoh, K., and H.C. Fibiger (1986) Cholinergic neurons of the laterodorsal tegmental nucleus: efferent and afferent connections. J. Comp. Neurol. *253:*277–302.

Schell, G.R., and P.L. Strick (1984) The origin of thalamic inputs to the arcuate premotor and supplementary motor areas. J. Neurosci. *4:*539–560.

Seki, M., and K. Zyo (1984) Anterior thalamic afferents from the mammillary body and the limbic cortex in the rat. J. Comp. Neurol. *229:*242–256.

Sharif, N.A., and J. Hughes (1989) Discrete mapping of brain mu and delta opioid receptors using selective peptides: Quantitative autoradiography, species differences and comparison with kappa receptors. Peptides *10:*499–522.

Shima, K., K. Aya, H. Mushiake, M. Inase, H. Aizawa, and J. Tanji (1991) Two movement-related foci in the primate cingulate cortex observed in signal-triggered and self-paced forelimb movements. J. Neurophysiol. *65:*188–202.

Sikes, R.W., and B.A. Vogt (1987) Afferent connections of anterior thalamus in rats: Sources and association with muscarinic acetylcholine receptors. J. Comp. Neurol. *256:*538–551.

Sikes, R.W., and B.A. Vogt (1991) Neuronal responses in cingulate cortex to noxious stimulation may originate in medial thalamus. Soc. Neurosci. Abstr. *17:*1561.

Sofroniew, M.V., J.V. Priestley, A. Consolazione, F. Eckenstein, and A.C. Cuello (1985) Cholinergic projections from the midbrain and pons to the thalamus in the rat, identified by combined retrograde tracing and choline acetyltransferase immunohistochemistry. Brain Res. *329:*213–223.

Sripanidkulchai, K., and J.M. Wyss (1986) Thalamic projections to retrosplenial cortex in the rat. J. Comp. Neurol. *254:*143–165.

Strick, P.L. (1985) How do the basal ganglia and cerebellum gain access to the cortical motor areas? Behav. Brain Res. *18:*107–123.

Tappaz, M.L., M.J. Brownstein, and M. Palkovits (1976) Distribution of glutamate decarboxylase in discrete brain nuclei. Brain Res. *108:*371–379.

Veazey, R.B., D.G. Amaral, and W.M. Cowan (1982) The morphology and connections of the posterior hypothalamus in the cynomolgus monkey (Macaca fascicularis). II. Efferent connections. J. Comp. Neurol. *207:*135–156.

Vogt, B.A. (1985) Cingulate cortex. In A. Peters and E.G. Jones (eds): Cerebral Cortex, Vol. 4. New York: Plenum Press, pp. 89–149.

Vogt, B.A., and D.L. Burns (1988) Experimental localization of muscarinic receptor subtypes to cingulate cortical afferents and neurons. J. Neurosci. *8:*643–652.

Vogt, B.A., and R.W. Sikes (1990) Lateral magnocellular thalamic nucleus in rabbits: Architecture and projections to cingulate cortex. J. Comp. Neurol. *299:*64–74.

Vogt, B.A., D.L. Rosene, and D.N. Pandya (1979) Thalamic and cortical afferents differentiate anterior from posterior cingulate cortex in the monkey. Science *204:*205–207.

Vogt, B.A., D.N. Pandya, and D.L. Rosene (1987) Cingulate cortex of the rhesus monkey: I. Cytoarchitecture and thalamic afferents. J. Comp. Neurol. *262:*256–270.

Vogt, B.A., R.W. Sikes, H.A. Swadlow, and T.G. Weyand (1986) Rabbit cingulate cortex: Cytoarchitecture, physiological border with visual cortex, and afferent cortical connections of visual, motor, postsubicular, and intracingulate origin. J. Comp. Neurol. *248:*74–94.

Vogt, B.A., M. Gabriel, L.J. Vogt, A. Poremba, E.L. Jensen, Y. Kubota, and E. Kang (1991) Muscarinic receptor binding increases in anterior thalamus and cingulate cortex during discriminative avoidance learning. J. Neurosci. *11:*1508–1514.

Vogt, B.A., P.B. Crino, and E.L. Jensen (1992) Multiple heteroreceptors on limbic thalamic axons: M_2 acetylcholine, serotonin$_{1B}$, beta$_2$adrenoceptors, mu opioid, neurotensin. Synapse *10:*44–53.

White, G.L., and D.D. Holmes (1976) A comparison of ketamine and the combination of ketamine-xylazine for effective surgical anesthesia in the rabbit. Lab. Anim. Sci. *26:*804–806.

Young, W.S. III, and M.J. Kuhar (1979) A new method for receptor autoradiography ^{3}H-opioid receptor labeling in mounted tissue sections. Brain Res. *179:*255–270.